

Jin-Seong Kim, Jae-Min Han, Mi-Ri Joung, Sang-Hyo Kweon, Chong-Yun Kang, Jong-Hoo Paik, Young-Hun Jeong and Sahn Nahm*

Ca_{0.15}Zr_{0.85}O_{1.85} Thin Film for Application to MIM Capacitor on Organic Substrate

Abstract: Ca_{0.15}Zr_{0.85}O_{1.85} (CSZ) films were grown on Pt/Ti/SiO₂/Si substrates at various temperatures using radio-frequency (RF) magnetron sputtering with a CaZrO₃ target. Crystalline CSZ phase was formed in the film grown even at room temperature (RT). For the film grown at 300°C, a dielectric constant (k) of value 27.6 and a low $\tan \delta$ of 0.005 were obtained at 100 kHz, and a similar k value of 26.7 with a high Q -value of 646 was obtained at 2.0 GHz. This film also showed a large capacitance density (264 nF/cm²), a small TCC (75 ppm/°C at 100 kHz), a low leakage current (1.44×10^{-8} A/cm² at 1.5 MV/cm), and a large breakdown field strength (2.25 MV/cm). Moreover, a 600 nm-thick CSZ film grown on polyimide substrate at RT satisfied all the ITRS 2016 requirements for a capacitor on an organic substrate. Therefore, the CSZ film, grown at a temperature $\leq 300^\circ\text{C}$, is a good candidate for use in embedded capacitors in printed circuit boards.

Keywords: calcia-stabilized zirconia, dielectric, embedded capacitor, RF sputtering, thin film

DOI 10.1515/ehs-2014-0010

*Corresponding author: Sahn Nahm, Department of Materials Science and Engineering, Korea University, 1-5 Ga, Anam-Dong, Seongbuk-Gu, Seoul 136-701, Korea; Information Technology-Nano Science, KU-KIST Graduate School of Converging Science and Technology, 1-5 Ga, Anam-Dong, Seongbuk-Gu, Seoul 136-713, Korea, E-mail: snahm@korea.ac.kr

Jin-Seong Kim: E-mail: foreverkjs@korea.ac.kr, Jae-Min Han:

E-mail: hjm3975@korea.ac.kr, Mi-Ri Joung:

E-mail: miri0806@korea.ac.kr, Sang-Hyo Kweon:

E-mail: petitzel1223@korea.ac.kr, Department of Materials Science and Engineering, Korea University, 1-5 Ga, Anam-Dong, Seongbuk-Gu, Seoul 136-701, Korea

Chong-Yun Kang, Information Technology-Nano Science, KU-KIST Graduate School of Converging Science and Technology, 1-5 Ga, Anam-Dong, Seongbuk-Gu, Seoul 136-713, Korea; Thin Film Materials Research Center, Korea Institute of Science and Technology, 39-1, Hawolgok-Dong, Seongbuk-Gu, Seoul 136-791, Korea, E-mail: cykang@kist.re.kr

Jong-Hoo Paik: E-mail: jhpaik@kicet.re.kr, Young-Hun Jeong:

E-mail: yhjeong@kicet.re.kr, Electronic Components Center, Korea Institute of Ceramic Engineering and Technology, Seoul 153-081, Korea

Introduction

To cope with the development of mobile electronic systems, the size of electronic devices must be reduced while their performance is simultaneously enhanced. To decrease the size of these devices, passive components such as capacitors, resistors, and inductors need to be embedded into printed circuit boards (PCBs) or low-temperature co-fired ceramic substrates (Gongora-Rubio et al. 2001; Bhattacharya and Tummala 2000; Park et al. 2006; Rahayu et al. 2013). Since the decoupling capacitor requires the most room in such electronic devices, investigations of methods for embedding decoupling capacitors have become more common. In addition, parasitic inductance can be reduced in an embedded capacitor compared with the surface-mounted capacitors. Therefore, the embedment of the decoupling capacitors in the PCB can provide both miniaturization and performance enhancements in the device (Maria et al. 2001; Ulrich 2004; Maeng et al. 2008; Tilmans, Raedt, and Beyne 2003; Kim et al. 2004; Kingon and Srinivasan 2005).

To embed the decoupling capacitor inside the PCB, the dielectric thin films need to be grown at low temperatures ($\leq 300^\circ\text{C}$). According to the International Technology Roadmap for Semiconductors (ITRS), for capacitors grown on organic substrates for future applications, the embedded decoupling capacitor should have the following properties by the year 2016: a capacitance larger than 5.0 nF/cm², a quality factor (Q -value) higher than 50 at radio-frequency (RF) range, and a breakdown voltage greater than 100 V (International Technology Roadmap for Semiconductors [ITRS] 2009).

Calcia-stabilized zirconia (CSZ) ceramics have a composition of Ca_{0.15}Zr_{0.85}O_{1.85}, in which Ca²⁺ ions replace some of the Zr⁴⁺ ions and stabilize the ZrO₂ cubic structure (Kingery et al. 1959; Patterson, Bogren, and Rapp 1967). CSZ ceramics are known as oxygen ion conductors because they contain many oxygen vacancies. Therefore, many investigations have been conducted on these ceramics to determine their suitability for electrolyte, oxygen sensors, solid-state battery, and solid oxide fuel cell applications (Kiukkola and Wagner 1957; Etsell and Flengas

1970; Chu and Seitz 1978; Pyun and Ihm 1982; Orliukas et al. 1993). However, the dielectric properties of CSZ ceramics have not yet been reported. According to our previous work, CSZ ceramics sintered at 1,400°C possessed a dielectric constant (k) value of 24–27 with a very low dielectric loss of 0.2% at 100 kHz (Kim 2013). Therefore, the CSZ ceramics appear to have the required dielectric properties for use in decoupling capacitors. Moreover, it is also possible that CSZ films have these desirable dielectric properties and can be employed in thin film embedded capacitors. In this work, CSZ films were grown under various conditions and their dielectric properties were characterized in order to determine their potential as embedded thin film capacitors.

Experimental procedure

The CSZ films were grown on a Pt/Ti/SiO₂/Si (Pt–Si) substrate by RF-magnetron sputtering of a 2-inch-diameter CaZrO₃ target. The target was synthesized at 1,500°C for 3 h using the conventional solid-state method. Deposition was carried over a temperature range extending from room temperature (RT) to 700°C in a mixed oxygen and argon (20/80) atmosphere with a total pressure of 5 mTorr. A sputtering power of 100 W was used for the deposition. In order to confirm the applicability of the CSZ film capacitor on organic substrates, a 600 nm-thick CSZ film was also grown at RT on a Pt/polyimide (Pt–PI) substrate.

The crystal structures of the films were examined by X-ray diffractometry (XRD; D/Max-2500/PC, Rigaku, Tokyo, Japan) and transmission electron microscopy (TEM; JEM-2100F, JEOL, Tokyo, Japan). The thin-film method, in which the incident angle of the X-ray was fixed at approximately 3° while the detector was rotated around 2 θ -axis, was used for the measurement of the XRD patterns of the films. The focused ion beam (FIB: Quanta 200 3D, FEI, Hillsboro, Oregon, USA) method was used for the preparation of the cross-sectional thin-film sample for TEM analysis. A compositional analysis was performed using energy dispersive spectroscopy (EDS; EMAX, Horiba, Kyoto, Japan) that is part of the equipment of the TEM. The Cliff–Lorimer method with k factors of Ca = 1.00793 and Zr = 1.87352 was used for the quantification of the chemical composition of the films. The microstructure and surface roughness of these films were analyzed by scanning electron microscopy (SEM; Hitachi S-4800, Hitachi High-Tech, Tokyo, Japan) and atomic force microscopy (AFM; Dimension 3100 Nanoman, Veeco, Santa Barbara, USA), respectively.

The interface between the CSZ film and the Pt electrode was analyzed by Auger electron spectroscopy (AES; Physical Electronic PHI 680 Auger electron spectroscopy, ULVAC-PHI, Inc., Chigasaki, Japan).

To measure the dielectric properties over the frequency range 75.0 kHz to 1.0 MHz, Pt was deposited on the CSZ films using conventional DC sputtering to form the top electrode of a metal-insulator-metal capacitor. After metal deposition, rapid thermal annealing was carried out at the growth temperature of each film for 5 min under the oxygen pressure of 5.0 Torr. The top electrode was patterned using a shadow mask to form a 380 μ m diameter disk. The capacitance and dissipation factor were measured using an LCR meter (Agilent 4285A, Agilent Technologies, Palo Alto, USA). To obtain the dielectric properties in the RF range, Al was deposited on the CSZ film as the top electrode using RF magnetron sputtering. The Al electrode was patterned to form a circular patched-capacitor structure by photolithography. The complex reflection coefficient was measured from 0.5 to 5 GHz by using a Vector Network Analyzer (Agilent (HP) 8510C Network Analyzer, Agilent Technologies, Palo Alto, USA). The k value and $\tan \delta$ were calculated from the two reflection coefficients of capacitors having different inner diameters but the same outer diameter (Ma et al. 1998; Lue, Tseng, and Huang 2002). The leakage current was measured using a programmable electrometer (Keithley 6517, Keithley Instruments, Inc., Cleveland, USA).

Results and discussion

Figure 1(a)–(e) shows the XRD patterns of the films grown at various temperatures by sputtering of a CaZrO₃ target. The crystalline CSZ phase was formed in all the films, even in the film grown at RT (Figure 1(a)). The CSZ phase remained in the films grown at higher temperatures, but the CaZrO₃ phase, which has the orthorhombic perovskite structure, was not present in these films. The film grown at RT shows random growth directions, but the films grown at high temperatures ($\geq 300^\circ\text{C}$) exhibited higher intensity (111) peak, indicating that these films grew in the preferred [111] direction. In addition, peaks of the Pt electrode appeared, as indicated by the arrows in Figure 1 (b) and (d), which arise from a slight tilt of the specimens when they were attached to the XRD sample holder.

To clarify the formation of the CSZ phase in the films, a TEM analysis was conducted on the films grown at RT and at 700°C. Figure 2(a) shows the bright-field image of the film grown at RT, and the inset shows the electron

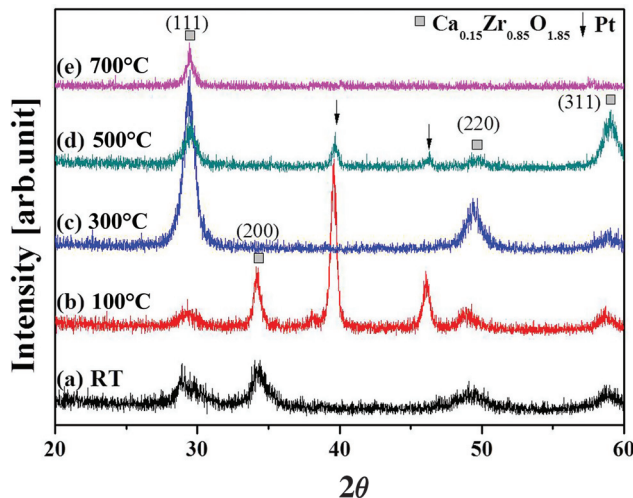


Figure 1 XRD patterns of the films grown at various temperatures: (a) RT, (b) 100°C, (c) 300°C, (d) 500°C, and (e) 700°C

diffraction pattern taken from this film. The film has a thickness of 125 nm and is well developed, with a sharp and continuous interface between the Pt electrode and film. Similar results were obtained from the films grown at higher temperatures. A ring-type electron diffraction

pattern, indexed as that of the CSZ phase, was obtained from this film, indicating that the small crystalline CSZ grains were formed in this film. A high-resolution TEM (HRTEM) image was also taken from this film, as shown in Figure 2(b). The inset of Figure 2(b) shows the fast Fourier transform (FFT) diffraction pattern calculated from the HRTEM image, and it corresponds to the (−110) electron diffraction pattern of the CSZ phase. These TEM results indicate that the crystalline CSZ phase was well formed in the film grown at RT. EDX analysis was also conducted on this film, as shown in Figure 2(c), and the chemical compositions of the film are shown in the inset. The ratio of Ca^{2+} to Zr^{4+} ions is approximately 1.0:4.9, confirming that the phase formed in the film grown at RT is the CSZ phase.

Figure 3(a) shows a HRTEM image of the film grown at 700°C, and the FFT diffraction pattern corresponding to the (−110) electron diffraction pattern of the CSZ phase is shown in the inset. These results indicate that the CSZ phase was well developed in this film. An EDX analysis was also conducted on this film, as shown in Figure 3(b) and the chemical compositions of the film are shown in the inset. The ratio between Ca^{2+} and Zr^{4+} ions is

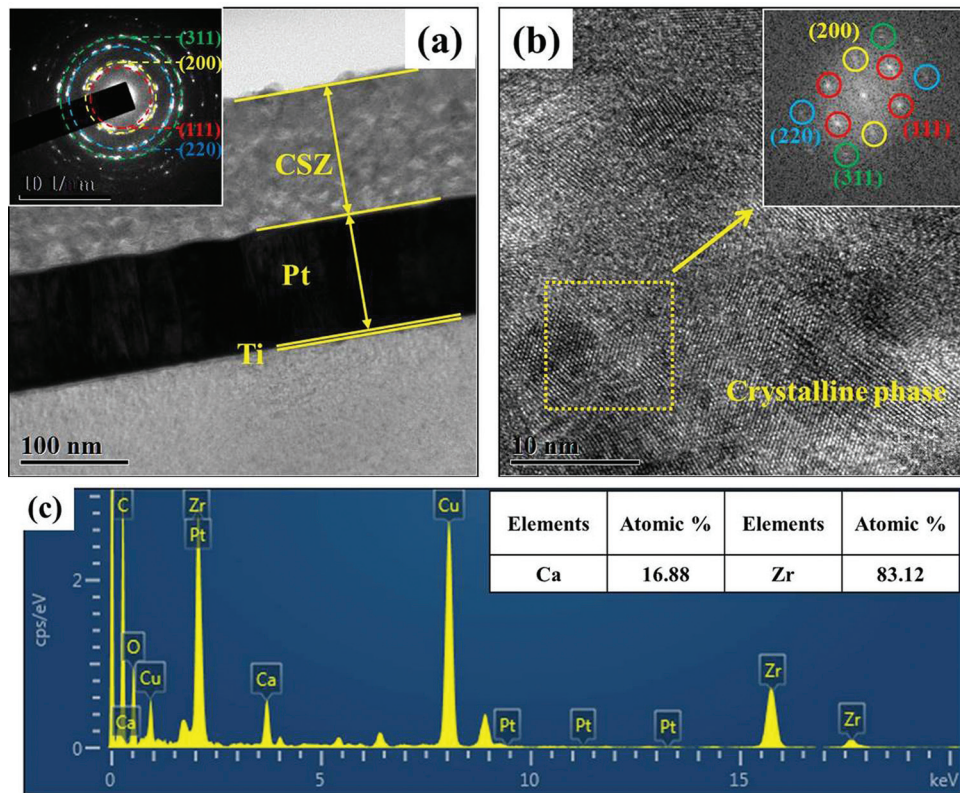


Figure 2 (a) Cross-sectional TEM bright-field image and the electron diffraction pattern, (b) HRTEM image and its FFT pattern, and (c) EDS spectrum and chemical composition of the CSZ film grown at RT

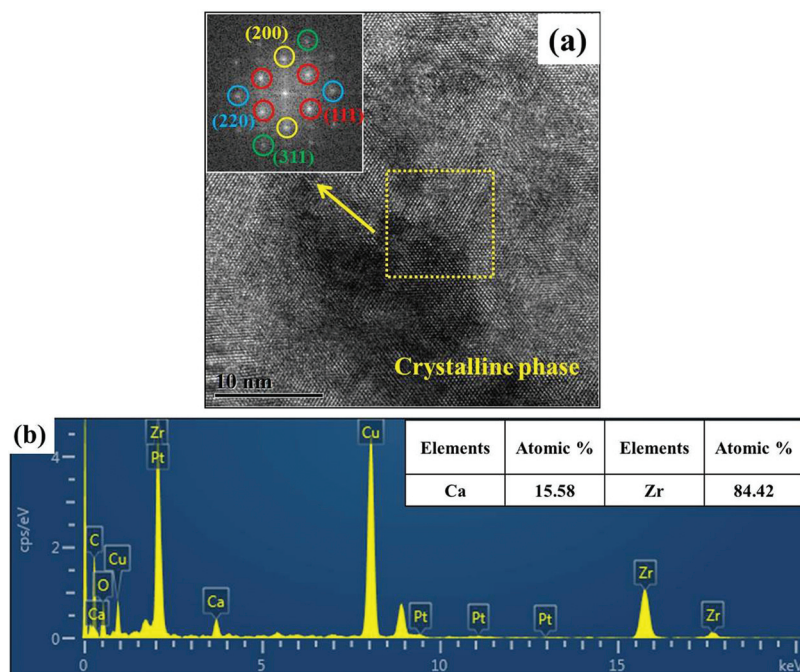


Figure 3 (a) HRTEM image and its FFT pattern and (b) EDS spectrum and chemical composition of the CSZ film grown at 700°C

approximately 1.0:5.4, which is similar to that of the film grown at RT. Therefore, the CSZ phase was also formed in the film grown at 700°C. It is interesting that the CaZrO_3 phase was not formed in these films. According to the previous work, for a film grown by pulsed laser deposition (PLD), the O_2 pressure during growth was important for the formation of the CaZrO_3 phase (Joseph et al. 2001). Although the same CaZrO_3 target was used for the deposition, the CaZrO_3 phase was formed in the film grown under high oxygen pressure, but the CSZ phase was formed in the film grown under low oxygen pressure (Joseph et al. 2001). In general, the oxygen partial pressure used in the sputtering process (≤ 10 mTorr) is much lower than that used in PLD (100–700 mTorr). Therefore, although the same CaZrO_3 target was used for the deposition, it might be very difficult to obtain the CaZrO_3 film using the RF sputtering method.

Figure 4(a)–(c) shows the AFM images of the CSZ films grown at various temperatures. The thickness of all films was approximately 100 nm. The root mean square value of the surface roughness (R_{rms}) of the film grown at 100°C is approximately 3.2 nm (Figure 4(a)), and a similarly rough surface was formed on the films grown at low temperatures ($\leq 100^\circ\text{C}$). Surface roughness decreased with increasing growth temperature, and the films grown at temperatures between 300°C and 500°C showed smooth surfaces with R_{rms} values of approximately 1.5 nm, as shown in Figure 4(b). However, R_{rms}

began to increase again when the growth temperature exceeded 500°C, and the film grown at 700°C exhibited a large R_{rms} of 3.9 nm. The Auger depth profiles of the film grown at 300°C are shown in Figure 4(d). No diffusion of Pt ions into the CSZ film, or of Ca, Zr, and O ions into the bottom Pt electrode, was detected, indicating the formation of a chemically sharp interface between the film and the Pt electrode. Similar results were obtained from the films grown at the other temperatures.

Figure 5(a) shows the variations in both k and the dissipation factor for the films grown at various temperatures as a function of frequency. The film grown at RT shows a small k value of 17.0 with a low dissipation factor of 2.3% at 100 kHz, and the variation of k with the frequency was negligible. The k value of the films increases with increasing growth temperature, up to 29.1 for the film grown at 700°C. This is probably to the result of increases in both grain size and crystallinity of the films grown at high temperatures (Uchino 2000). A high k value of 27.6 and a low dissipation factor of 0.5% were obtained at 100 kHz for the film grown at 300°C. Figure 5(b) shows the variation in the capacitance density of the films grown at various temperatures with respect to the applied voltage measured at 100 kHz. A capacitance density of 124 nF/cm² was obtained for the film grown at RT, and this increased to 264 nF/cm² for the film grown at 300°C, which is the maximum growth temperature possible for applications involving devices on organic substrates.

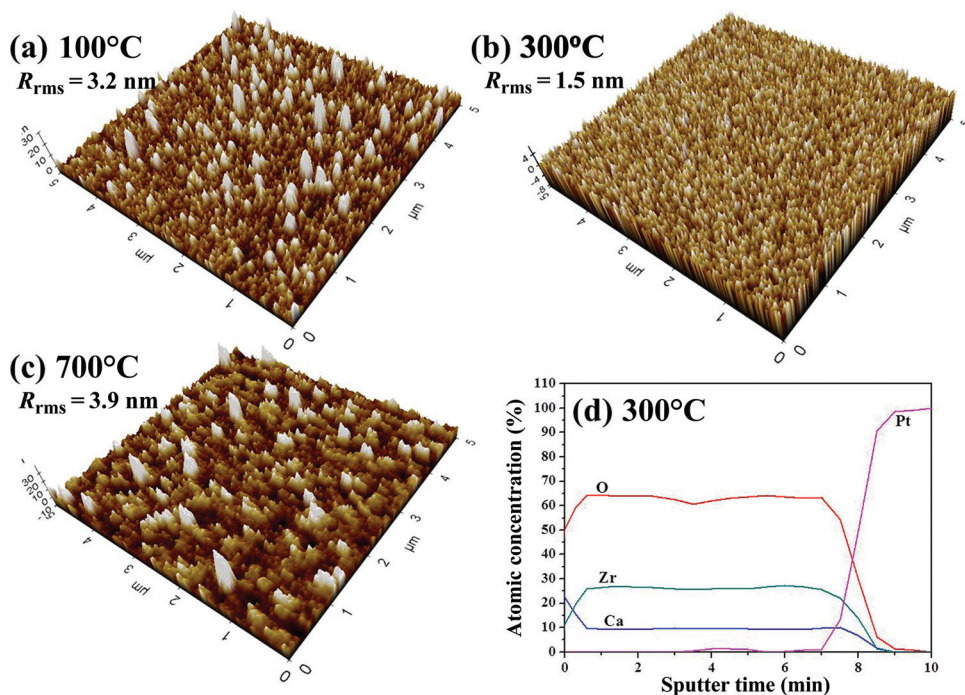


Figure 4 AFM images of CSZ films grown at various temperatures: (a) 100°C, (b) 300°C, and (c) 700°C. (d) Auger depth profile of the CSZ film grown at 300°C

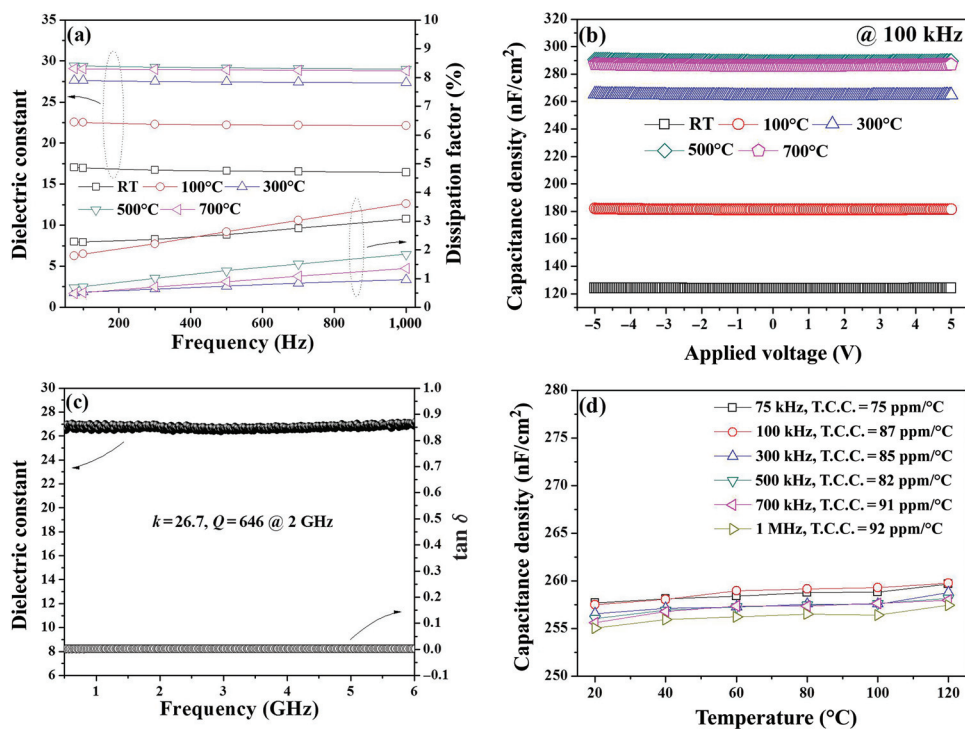


Figure 5 (a) k values and dissipation factors and (b) variation in the capacitance density with respect to the voltage for the CSZ films grown at various temperatures, measured at various frequencies. (c) k values and $\tan \delta$ values measured at RF frequencies, and (d) variation of the capacitance density measured at various frequencies as a function of temperature for the CSZ film grown at 300°C

According to the ITRS of 2009, the capacitance density of a capacitor on an organic substrate is required to be greater than 5.0 nF/cm^2 by 2016 (International Technology Roadmap for Semiconductors (ITRS) 2009). Therefore, the capacitance densities of the films reported here, even those grown at RT, satisfy the ITRS requirement. The dielectric properties of the film grown at 300°C were also measured in the RF range, as shown in Figure 5(c). The k value of the film was 26.7 at 2 GHz, which is similar to the k value measured at low frequency. Furthermore, it exhibits a very high Q -value of 646 at 2.0 GHz. According to the ITRS, Q -value for a capacitor formed on an organic substrate needs to be larger than 50 by 2016, a condition which is satisfied by this film. The temperature coefficient of capacitance (TCC) of the CSZ film grown at 300°C was also measured at various frequencies, as shown in Figure 5(d). This film showed a very low TCC of 75 ppm/ $^\circ\text{C}$ at 75 kHz, and this increased slightly with increasing frequency to 92 ppm/ $^\circ\text{C}$ at 1.0 MHz. According to the ITRS, the TCC value for a capacitor grown on an organic substrate should be less than 300 ppm/ $^\circ\text{C}$, indicating that the TCC value of this CSZ film satisfies the ITRS requirement for 2016.

The leakage current densities of the CSZ films grown at various temperatures are shown in Figure 6. The leakage current density of the film grown at RT is large, and the leakage current density decreases with increasing growth temperature. For the film grown at 300°C , a very low leakage current density of $1.44 \times 10^{-8} \text{ A/cm}^2$ at 1.5 MV/cm and a high breakdown field of 2.25 MV/cm were obtained. Similar results were observed for the film grown at 500°C . However, for the film grown at 700°C ,

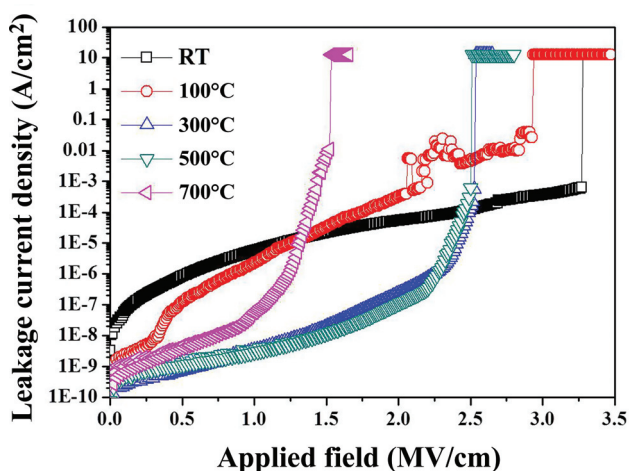


Figure 6 Leakage current densities of the CSZ films grown at various temperatures

the electrical properties were degraded, and it exhibited increased leakage current density and decreased breakdown voltage. Variation in the electrical properties of the CSZ films follows the variation of the surface roughness (Figure 4(a)-(c)). Since the top electrode is formed on top of the surface of the film, the interface between top electrode and film is not well formed if the surface roughness of the film is large, resulting in the degradation of the electrical properties of the film. Therefore, it is generally accepted that the electrical properties of a film are influenced by its surface roughness (Cho et al. 2009; Kim et al. 2013). Moreover, the low leakage current density with the high breakdown voltage for the films grown at 300 and 500°C could be explained by their small surface roughness.

According to the ITRS, the breakdown voltage of the film should be greater than 100 V (International Technology Roadmap for Semiconductors (ITRS) 2009). Since the thickness of the film grown at 300°C is approximately 95 nm with a breakdown voltage of 22.5 V, the breakdown voltage requirement of 100 V could be satisfied for a CSZ film thicker than 500 nm. A 600 nm-thick CSZ film was grown at RT on a Pt-PI substrate to confirm the applicability of the CSZ film capacitor on organic substrates, as shown in Figure 7(a). The CSZ film is well developed, with a sharp and continuous interface between the Pt electrode and film. Figure 7(b) shows the variations in both k and the dissipation factor of this film as a function of frequency. This film shows a k value of 17.5 with a low dissipation factor of 2.0% at 100 kHz, which are similar to those of a CSZ film grown on the Pt-Si substrate at RT (see Figure 5(a)). The variation of k with the frequency was negligible. Figure 7(c) shows the variation in the capacitance density of the 600 nm-thick CSZ film with respect to the applied voltage, measured at various frequencies. A capacitance density of 26.8 nF/cm^2 was obtained for the film, which is larger than the required capacitance density of a capacitor on an organic substrate by the 2016 standards ($>5.0 \text{ nF/cm}^2$). The leakage current density of the 600 nm-thick CSZ film is also shown in Figure 7(d). A low leakage current density of $9.5 \times 10^{-7} \text{ A/cm}^2$ at 50.0 V (0.83 MV/cm) and a high breakdown voltage of 184 V were obtained. According to the ITRS, the breakdown voltage of the film should be greater than 100 V (International Technology Roadmap for Semiconductors (ITRS) 2009) and the 600 nm-thick CSZ film grown on PI substrate at RT satisfied this requirement. Therefore, the 600 nm-thick CSZ film grown on Pt-PI substrate satisfied all the ITRS 2016 requirements for a capacitor on an organic substrate.

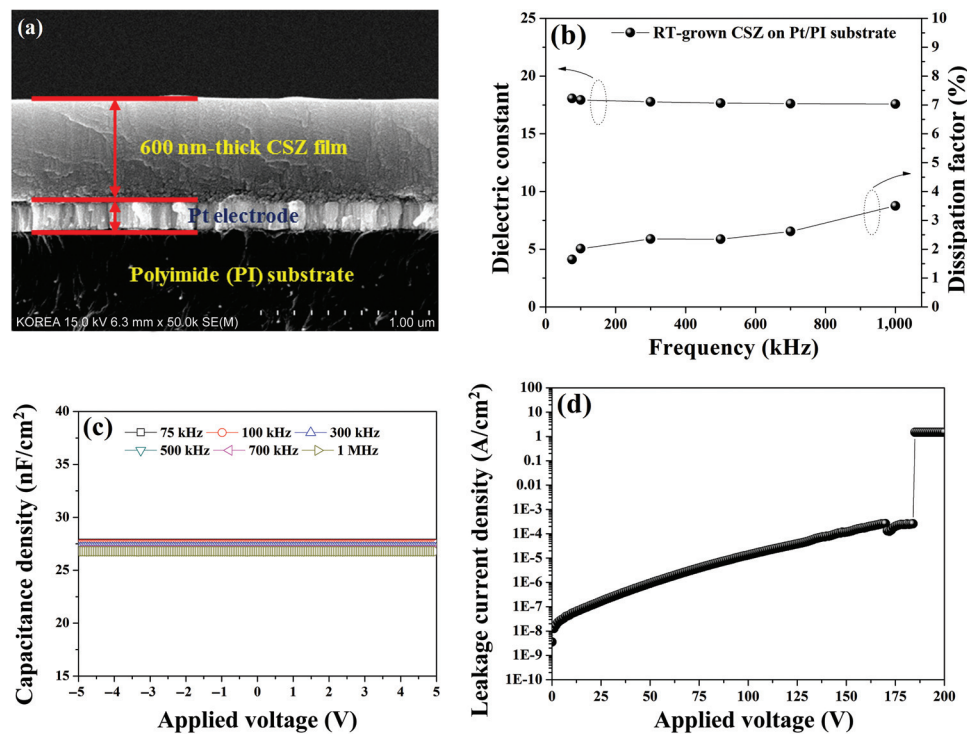


Figure 7 (a) SEM image, (b) k values and the dissipation factor, (c) the capacitance density, and (d) leakage current densities for the 600 nm-thick CSZ film grown on Pt/PI substrate at RT

Conclusions

Calcium-stabilized zirconia films were grown on Pt–Si substrates using RF sputtering with a CaZrO_3 ceramic target. Formation of the CSZ film could be explained by the low oxygen partial pressure during growth. The crystalline CSZ films were high quality, exhibiting continuous and sharp interfaces with the substrates, even when grown at RT. The R_{rms} value of the film was small (~ 1.5 nm) for the films grown at 300 and 500°C, but the films grown at other temperatures showed larger surface roughness. For the film grown at 300°C, a k value of 27.6 and a low $\tan \delta$ of 0.005 were obtained at 100 kHz, and a similar k value of 26.7 with a high Q -value of 646 was obtained at 2.0 GHz. Moreover, the CSZ film grown at 300°C showed a large capacitance density (264 nF/cm^2), a small TCC ($75 \text{ ppm/}^\circ\text{C}$ at 100 kHz), a low leakage current ($1.44 \times 10^{-8} \text{ A/cm}^2$ at 1.5 MV/cm), and a large breakdown field strength (2.25 MV/cm). Furthermore, a 600 nm-thick CSZ film grown on Pt–PI substrate at RT satisfied all the ITRS 2016 requirements for a capacitor on an organic substrate, indicating that this film is a good candidate for embedded capacitor applications.

Acknowledgment: This work was supported by the Industrial Strategic Technology Development Program, 10041232, “Development of synthesis method of exfoliated inorganic nanosheets with a high dielectric constant of >300 and the corresponding thin films applicable for the fabrication of high performance MLCC” funded by the Ministry of Knowledge Economy (MKE, Korea).

References

- Bhattacharya, S. K., and R. R. Tummala. 2000. “Next Generation Integral Passives: Materials, Processes, and Integration of Resistors and Capacitors on PWB Substrates.” *Journal of Materials Science: Materials in Electronics* 11:253.
- Cho, K. H., T. G. Seong, J. Y. Choi, J. S. Kim, S. Nahm, C. Y. Kang, S. J. Yoon, and J. H. Kim. 2009. “Electrical Properties of $\text{Bi}_5\text{Nb}_3\text{O}_{15}$ Thin Film Grown on $\text{TiN}/\text{SiO}_2/\text{Si}$ at Room Temperature for Metal–Insulator–Metal Capacitors.” *IEEE Electron Device Letters* 30:614.
- Chu, S. H., and M. A. Seitz. 1978. “The Ac Electrical Behavior of Polycrystalline $\text{ZrO}_2\text{-CaO}$.” *Journal of Solid State Chemistry* 23:297.
- Etsell, T. H., and S. N. Flengas. 1970. “Electrical Properties of Solid Oxide Electrolytes.” *Chemical Reviews* 70:339.
- Gongora-Rubio, M. R., P. Espinoza-Vallejos, L. Sola-Laguna, and J. J. Santiago-Aviles. 2001. “Overview of Low Temperature

- Co-Fired Ceramics Tape Technology for Meso-System Technology (MsST).” *Sensors and Actuators A: Physical* 89:222. International Technology Roadmap for Semiconductors (ITRS). 2009. 2009 Edition. <http://www.itrs.net/Links/2009ITRS/Home2009.htm>
- Joseph, M., N. Sivakumar, P. Manoravi, and S. Vanavaramban. 2001. “Preparation of Thin Film of CaZrO_3 by Pulsed Laser Deposition.” *Solid State Ionics* 144:339.
- Kim, J. S.. 2013 “Oxide Thin Films Grown at Low Temperature for Application to Embedded Decoupling Capacitors.” Ph.D. Thesis, Korea University, Seoul, February 2013.
- Kim, J. S., M. G. Kang, S. H. Kweon, G. Han, C. Y. Kang, J. R. Yun, Y. H. Jeong, J. H. Paik, and S. Nahm. 2013. “Electrical Properties of Amorphous BaTi_4O_9 Films Grown on $\text{Cu/Ti/SiO}_2/\text{Si}$ Substrates Using RF Magnetron Sputtering.” *Journal of the American Ceramic Society* 96:1248.
- Kim, T., A. I. Kingon, J. P. Maria, and R. T. Croswell. 2004. “Ca-Doped Lead Zirconate Titanate Thin Film Capacitors on Base Metal Nickel on Copper Foil.” *Journal of Materials Research* 19:2841.
- Kingery, W. D., J. Pappis, M. E. Doty, and D. C. Hill. 1959. “Oxygen Ion Mobility in Cubic $\text{Zr}_{0.85}\text{Ca}_{0.15}\text{O}_{1.85}$.” *Journal of the American Ceramic Society* 42:393.
- Kington, A. I., and S. Srinivasan. 2005. “Lead Zirconate Titanate Thin Films Directly on Copper Electrodes for Ferroelectric, Dielectric and Piezoelectric Applications.” *Nature Materials* 4:233.
- Kiukkola, K., and C. Wagner. 1957. “Measurement on Galvanic Cells Involving Solid Electrolytes.” *Journal of the Electrochemical Society* 104:379.
- Lue, H. T., T. Y. Tseng, and G. W. Huang. 2002. “A Method to Characterize the Dielectric and Interfacial Properties of Metal–Insulator–Semiconductor Structures by Microwave Measurement.” *Journal of Applied Physics* 91:5275.
- Ma, Z., A. J. Becker, P. Polakos, H. Huggins, J. Pastalan, H. Wu, K. Watts, Y. H. Wong, and P. Mankiewicz. 1998. “RF Measurement Technique for Characterizing Thin Dielectric Films.” *IEEE Transactions on Electron Devices* 45:1811.
- Maeng, J., S. Song, N. Jeon, C. S. Yoo, H. Lee, and K. Seo. 2008. “Embedded Decoupling Capacitors up to 80 nF on Multichip Module-Deposited with Quasi-Three-Dimensional Metal–Insulator–Metal Structure.” *Japanese Journal of Applied Physics* 47:2535.
- Maria, J. P., K. Cheek, S. Streiffer, S. H. Kim, G. Dunn, and A. Kingon. 2001. “Lead Zirconate Titanate Thin Films on Base-Metal Foils: An Approach for Embedded High-Permittivity Passive Components.” *Journal of the American Ceramic Society* 84:2436.
- Orliukas, A., P. Bohac, K. Sasaki, and L. Gauckler. 1993. “Relaxation Dispersion of Ionic Conductivity in a $\text{Zr}_{0.85}\text{Ca}_{0.15}\text{O}_{1.85}$ Single Crystal.” *Journal of the European Ceramic Society* 12:87.
- Park, J. H., W. S. Lee, N. J. Seong, S. G. Yoon, S. H. Son, H. M. Chung, J. S. Moon, H. J. Jin, S. E. Lee, J. W. Lee, et al. 2006. “Bismuth-Zinc-Niobate Embedded Capacitors Grown at Room Temperature for Printed Circuit Board Applications.” *Applied Physics Letters* 88:192902.
- Patterson, J. W., E. C. Bogren, and R. A. Rapp. 1967. “Mixed Conduction in $\text{Zr}_{0.85}\text{Ca}_{0.15}\text{O}_{1.85}$ and $\text{Th}_{0.85}\text{Y}_{0.15}\text{O}_{1.925}$ Solid Electrolytes.” *Journal of the Electrochemical Society* 114:752.
- Pyun, S. I., and Y. E. Ihm. 1982. “Electrical Conduction of Partially Stabilized Zirconia $\text{Zr}_{0.94}\text{Ca}_{0.06}\text{O}_{1.94}$ as a Function of Temperature and Oxygen Partial Pressure.” *Journal of Materials Science* 17:2577.
- Rahayu, R., M. G. Kang, Y. H. Do, J. H. Hwang, C. Y. Kang, and S. J. Yoon. 2013. “Electrical Characteristics of $\text{Ba}_{0.6}\text{Sr}_{0.4}\text{TiO}_3$ Thin-Film Chip Capacitors for Embedded Passive Components.” *IEEE Electron Device Letters* 34:99.
- Tilmans, H., W. D. Raedt, and E. Beyne. 2003. “MEMS for Wireless Communications: ‘From RF-MEMS Components to RF-MEMS-SiP’.” *Journal of Micromechanics and Microengineering* 13:S139.
- Uchino, K., ed. 2000. *Ferroelectric Devices*, 1st ed. New York: Marcel Dekker.
- Ulrich, R. 2004. “Embedded Resistors and Capacitors for Organic-Based Sop.” *IEEE Transactions on Advanced Packaging* 27:326.